Eur. Phys. J. D (2020) 74: 64
https://doi.org/10.1140/epjd/e2020-100540-3

THE EUROPEAN PHYSICAL JOURNAL D

Regular Article

Low-pressure DC breakdown in alcohol vapours*

Jelena Sivoš[1,a], Dragana Marić[1], Gordana Malović[1], and Zoran Lj. Petrović[1,2]

[1] Institute of Physics, University of Belgrade, Pregrevica 118, 11080 Belgrade, Serbia
[2] Serbian Academy of Sciences and Arts, Knez Mihailova 35, 11001 Belgrade, Serbia

Received 29 October 2019 / Received in final form 24 January 2020
Published online 1 April 2020

Abstract. The results covered in this paper provide breakdown data represented by Paschen curves for methanol, isopropanol and n-butanol, along with the corresponding axial profiles of emission in Townsend regime of the discharge and including the optical emission spectra. Paschen curves were recorded in the range of *pd* (pressure x electrode gap) from 0.10 to 3.00 Torr cm. The optical emission spectra (OES) are recorded for wavelength range from 300 to 900 nm, for discharges in all studied alcohols. The recorded spectra enabled identification of species that participate in these discharges. All three alcohols exhibit emission from excited radicals OH (at 306.4 nm), CH (at 431.2 nm) and Hα (at 656.4 nm) produced mostly in dissociative excitation by electrons. Recorded profiles of emission enabled us to identify conditions where processes induced by heavy particles (ions and fast neutrals) are dominant in inducing emission from the discharge.

1 Introduction

Alcohols are organic compounds that are widely used in numerous applications. In recent years, with increasing public awareness of the need for environmental protection, and the reduction of greenhouse gas emissions in the fight against global warming, eco-friendly and renewable energy sources have attracted attention. Certainly, hydrogen is one of the most promising fuels and clean energy sources, however, the main problem is its storage, due to the low density. One of the solutions is to obtain it directly on-site from other compounds. Alcohols have proven to be particularly attractive and suitable for hydrogen production using low-temperature non-equilibrium plasmas [1–4]. It has been proposed that Direct Alcohol Fuel Cells (PEMFC fuel cells) may be used in vehicles, but also in other portable electric or electronic devices [5–8]. In relation to the use of alcohols as a fuel or as its precursor, studies of combustion and initialization of the discharge are needed.

Further development of environmentally friendly energy sources requires an improvement of existing materials and obtaining new ones with enhanced characteristics such as technologies to prepare materials required to grow nanostructures for fuel cells (for example [8–10]). Carbon nanomaterials, such as nanotubes and graphene, are very interesting for a wide variety of applications due their unique structure and exceptional electrical, physical and morphological properties. Specifically, one of the most prominent features of graphene is its high conductivity, which makes it attractive as a material for channels in the next generation of ultra-fast transistors and for transparent electrodes in solar cells. Many studies have shown that plasmas in alcohols can be used as a carbon source [11–15]. It turns out that hydroxyl groups and oxygen atoms from alcohol play an important role in crystallization and formation of nanographene layers [14].

Another important application within the context of gas discharges is in elementary particle/ionizing radiation detection, where alcohol vapours and other hydrocarbon gases are used as quenchers [16–19]. In some cases, alcohols are also applied to suppress aging of detectors [20]. Even though alcohols are used in small percentages in gaseous detectors, in mixtures with atomic buffer gases, they have a critical influence on the shape of electron energy distribution and transport coefficients, due to large vibrational excitation cross sections [21,22].

Thus, there is a versatile field of application of these non-equilibrium discharges, both in liquid state or as a vapour. The development of future and improvement of existing applications are based on a good understanding of elementary processes that take place in the discharges. A special challenge is to extend the techniques and understanding of the gas phase discharges into the realm of discharges in liquids, liquid-gas interfaces and gas mixtures involving vapours [23]. The information, on fundamental

* Contribution to the Topical Issue "Low-Energy Positron and Positronium Physics and Electron-Molecule Collisions and Swarms (POSMOL 2019)", edited by Michael Brunger, David Cassidy, Saša Dujko, Dragana Marić, Joan Marler, James Sullivan, Juraj Fedor

[a] e-mail: sivosj@ipb.ac.rs

processes, can be obtained from measurements of elementary properties of discharges such as breakdown, operating regimes, discharge anatomy, etc. Hence, the importance of breakdown studies lays in the fact that they can reveal information on individual processes and their balance in discharges [24–30].

Back at the beginning of the twentieth century, Townsend had formulated the theory of initiation of electrical breakdown in a gas [29,30], which predicts that the breakdown voltage (V_b) scales with the pd product, where d represents the length of the electrode gap and p is the pressure. Product pd is proportional to the number of collisions that one particle makes while covering some distance. A Paschen curve (plot of the breakdown voltage dependence on pd), is unique to each gas or gas mixture and provides information for a better understanding of the underlying processes in electrical breakdown. Our research aims at providing some of the basic data on a breakdown and various operation regimes of low-pressure DC discharges in vapours of liquids (water and alcohols) [27,28,31]. The lack of such data in the literature is one of the key reasons why it is necessary to address this type of research.

In this paper, we present measurements of the Paschen curves obtained for the discharges in the vapours of primary alcohols (methanol and n-butanol) and secondary alcohol (isopropanol) at low–pressures and compared to previously published results for ethanol [31]. All measurements of electrical properties are supported by recordings of axial discharge profiles by an ICCD camera. Therefore, our study of low–pressure discharges in alcohol vapors provides a complete set of breakdown data together with spatial emission profiles of the low–current discharges. Such sets may be the basis for further analysis or may be employed directly (e.g. ionization coefficients) [22,24,32]. The present measurements can also provide new or give additional insight into the understanding of relevant atomic and surface processes associated with electrical breakdown [24,33,34].

2 Experimental setup

The electrode system consists of two flat electrodes 5.4 cm in diameter and is placed inside a tightly fitted quartz tube. The distance between electrodes is adjustable and the present measurements were performed in a plane-parallel electrode geometry, at two different electrode distances: 1.1 and 3.1 cm. The cathode is made of copper, while the anode is a quartz window with a deposited thin, transparent, conductive platinum film. A simplified schematic of the experimental set-up is provided at Figure 1.

The discharge chamber construction allows side–on recordings and we used two setups to register emission coming from the discharge. In the first case, the camera was equipped with a glass lens allowing us to acquire axial discharge profiles of the spectrally integrated emission in the visible range of spectra, defined by the transparency of the lens and the quantum efficiency of the ICCD photocathode. For spectrally resolved measurements we used

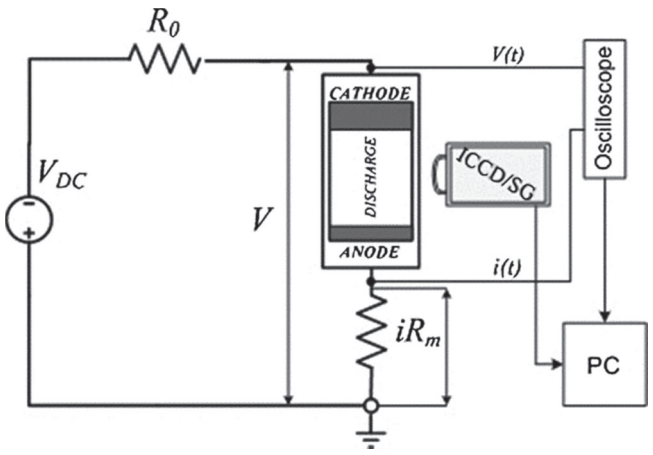

Fig. 1. Schematics of the experimental setup and the electrical circuit used in measurements. All the recordings were made with an ICCD camera mounted with an objective lens, a filter or a spectrograph (SG). The series resistor R_0 is used to limit current and keeps it as low as possible for measurements in the Townsend discharge. R_m is the "monitoring" resistor used to measure discharge current.

band–pass optical filters in front of the lens thus enabling recordings of emission profiles for a narrow range of wavelengths. In another setup, optical spectrum of emission from alcohol vapour discharges was recorded by focusing light from the discharge to a 100 μm entrance slit of the ORIEL MS127i spectrograph. In both cases sensitive ICCD camera (Andor IStar DH720-18U-03) was used to detect the signal. The spectrograph is equipped with a ruled grating with a wavelength range from 200 to 1200 nm with spectral resolution 0.22 nm. A more detailed description of the experimental procedure is given in [31]. The requirements of the experiment (very small currents, steady state Townsend discharges) dictated the need to limit the resolution in order to increase the sensitivity.

The vacuum chamber is pumped down to the base pressure of below 10^{-6} Torr. Prior to the measurements, the surface of the cathode is treated by a relatively high current discharge in hydrogen (30 μA), approximately 30 min, until a stable voltage is achieved. The cathode surface treatment can remove oxide layers and impurities from the cathode, up to an extent where the surface becomes stable during the long periods of measurements. This procedure has been proven to provide reliable and reproducible breakdown data [24,33]. After the cleaning of the cathode, the discharge chamber is again vacuumed to the pressure of around 10^{-6} Torr. Both, treatment in hydrogen discharge and measurements in alcohol vapours are done in a slow flow regime, to ensure that possible impurities formed in the discharge chamber are continuously removed.

We have performed measurements for three primary alcohols: methanol, ethanol (see our earlier paper [31]) and n-butanol, and one secondary alcohol – isopropanol (2–propanol). The vapours are obtained from 99.5% purity methanol, isopropanol, and n-butanol. Water is an abundant impurity in alcohols (max. 0.2%), while other volatile impurities such as acetone, aldehydes and formic acid (max. 0.002%) are present in small quantities. Also, iron

(0.0005%) and some non-volatile substances (<0.001%) are present only in traces. Therefore, a small percentage of water vapour may be found in the discharge. Effects of inherent gas impurities can be critical in two cases. First, it is known that breakdown data in atomic gases are sensitive to molecular impurities, due to significant vibrational energy losses introduced by molecular gases. Second, the attachment to impurities may strongly affect discharges in gases that are not subject to attachment. In that respect dissolved oxygen would be the most important impurity. However, neither of the two possible processes are expected to affect strongly the results for gas discharges where ionization is a key process and is dominated by the most abundant gas. Therefore, water will not affect the results strongly (beyond its percentage abundance) through either of the two effects and the same is true for all other present components. Also, it should be stated that even without evaporating the dissolved oxygen it would not affect the breakdown potential and other properties of the discharge as the operating point is defined by the ionization to the most abundant gas i.e. alcohols.

The alcohol vapour is introduced into the discharge chamber from a test tube with a liquid sample, through a pressure regulating valve. Immediately after opening the valve, alcohol begins to boil due to the pressure difference above its surface (10^{-6} Torr) and the pressure of dissolved gases in the sample itself. In this way, alcohol becomes devoid of dissolved volatile constituents. The impurities are reduced in the liquid sample to a minimum throughout the boiling and vacuuming processes. Boiling stops when a significant part of volatile impurities evaporates. After boiling has ceased vapour is maintained at a moderate pressure (lower than the vapour pressure) in the chamber for period of 1–2 h in order to saturate the electrodes and the chamber walls. The vapour pressures of methanol, isopropanol and n-butanol at room temperature (25°C), are around 127, 44 and 7 Torr, respectively [35], so during the measurements operating pressures are kept well below these values to avoid the formation of liquid droplets.

The electric circuit is designed (as explained in greater detail in our previous papers [28,31,36]) to provide stable operation of the discharge near the breakdown conditions. The breakdown voltage for each *pd* is determined from the low–current limit of the discharge, by extrapolating the discharge voltage to zero current in the dark Townsend discharge mode [31,33,37].

3 Results and discussion

3.1 Paschen curves–breakdown data

Figure 2 shows breakdown voltage as a function of *pd*, where p is the pressure, and d is the electrode gap size. These measurements have been performed at two inter-electrode distances: 1.1 and 3.1 cm and cover the range of *pd*s from 0.10 to 3.00 Torr cm overlapping with the minimum of the breakdown voltage in all cases. The dashed lines in the graphs indicate the values of the reduced electric field E/N ($1\,\mathrm{Td} = 10^{-21}\,\mathrm{Vm}^2$). Shapes of Paschen curves for all alcohols are typical for gaseous low-pressure DC discharges [33]. Electrode gaps are measured to better than 2% uncertainty, pressure and voltage to better than 1%, which makes them too small to be presented in graphs.

The minimum of Paschen curve, in the case of methanol for the gap of 3.1 cm lies at 0.40 Torr cm, while breakdown voltage is 433 V. At the same gap, for isopropanol and n-butanol, the minimum lies at 0.30 Torr cm and breakdown voltages are 420 V and 415 V respectively. When distance between electrodes is 1.1 cm minimal breakdown voltages are: 455 V at 0.40 Torr cm for methanol, 436 V at 0.30 Torr cm for isopropanol, and 434 V at 0.25 Torr cm for n-butanol. Breakdown in ethanol vapour has been presented in detail in [31]. In Figure 2d we compare Paschen curves for ethanol with other studied alcohols. One may notice a general trend that the minimum of the Paschen curves shifts to lower voltages and lower *pd*, as one goes from simple to more complex alcohols. As molecule becomes more complex (more atoms) there are more modes for vibrational excitation (and vibrational excitation is the dominant process controlling the mean energy of the discharge) and thus losses are likely to be greater requiring breakdown at higher E/N. To the right of the Paschen minimum one can reach greater E/N by increasing the breakdown voltage and as a result the Paschen curve for the most complex molecule is above those that are less complex. To the left of the Paschen minimum the more efficient way to reach higher E/N (ie mean energy) is to shift the minimum to the lower values of *pd* as the values of the voltages for the minimums are similar. Thus the most complex molecule has the lowest breakdown voltage to the left of Paschen minimum.

Paschen curves (Fig. 2) obtained at different electrode gaps show good agreement at low E/N values (the right-hand branch of the Paschen curve). At higher E/N (the left-hand branch of the Paschen curve), some discrepancies in breakdown voltages at different electrode gaps are noticeable. The differences in breakdown voltages at different gaps may originate from slight pressure variations, which can have a large impact in a region of the steep rise of the curve. More importantly, processes at surfaces (secondary electron emission) have a stronger effect at high E/N, while low E/N breakdown is dominated by gas phase processes [24]. Even the slightest changes at cathode surface between two sets of measurements can be detected through differences in the left-hand branch of the Paschen curve. The applied experimental technique, in our measurements, is designed to ensure minimal discrepancies between different sets of measurements.

After the breakdown, discharge is stable at low-current (around $1\,\mu$A) up to $pd = 0.70$ Torr cm, except for n-butanol where the boundary is at 0.40 Torr cm. Above these values discharge ignites into oscillations. At higher *pd* we obtain periodic relaxation oscillations from which we can determine the breakdown voltages [38–41]. In the case of alcohol discharges these periodic relaxation oscillations have frequencies between 250 and 890 Hz. However, above 3.0 Torr cm, it becomes difficult to control the discharge, oscillations become random and we cannot use them to establish breakdown voltage with reasonable accuracy. At

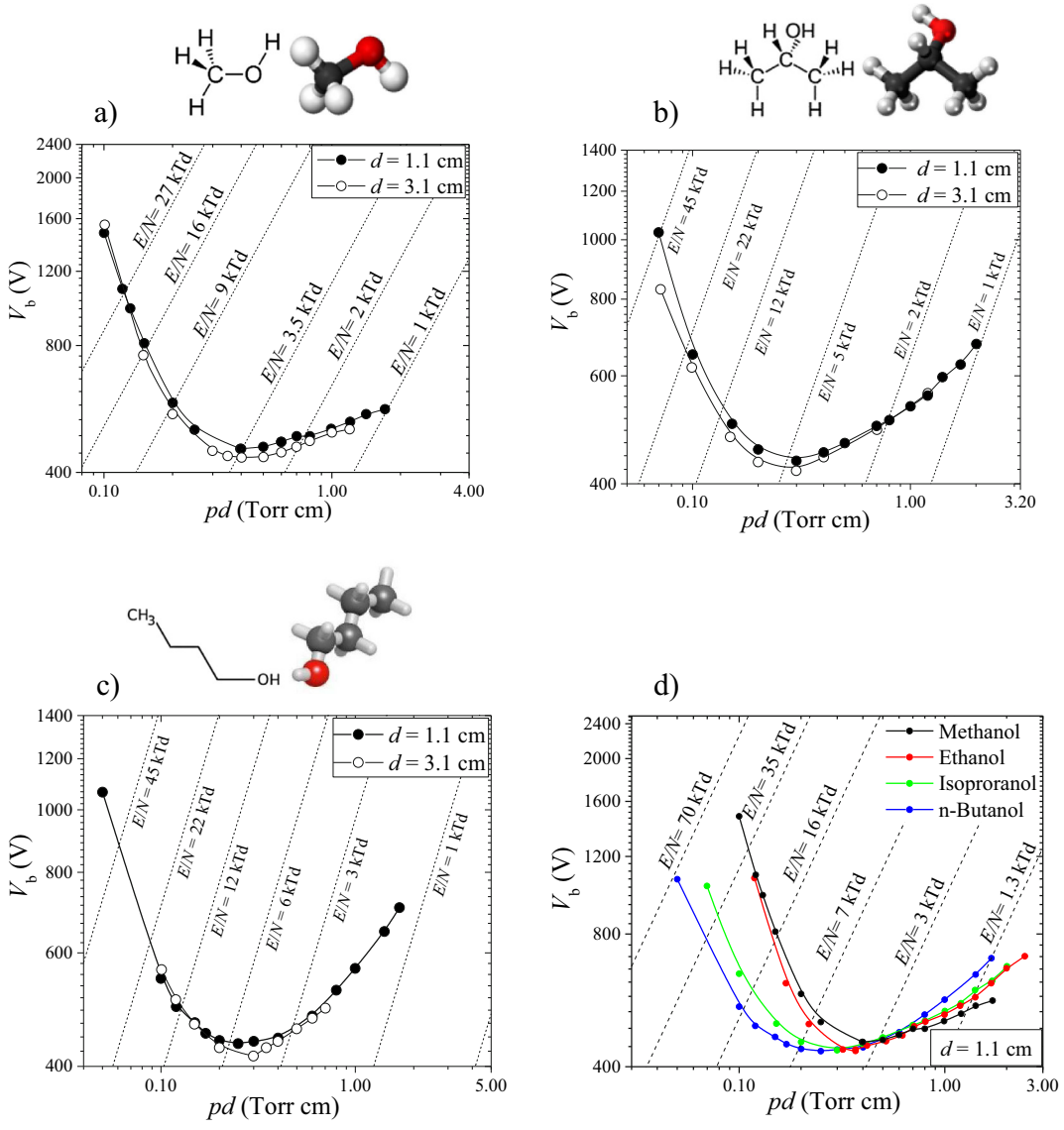

Fig. 2. Paschen curves for discharges in vapours of alcohols, at various reduced electric field (E/N) indicated by dashed lines [$1\,\mathrm{Td} = 10^{-21}\,\mathrm{Vm}^2$ and $1\,\mathrm{Torr} = 133.32\,\mathrm{Pa}$]. (a) Methanol vapour at $d = 1.1\,\mathrm{cm}$ (full circles) and at $d = 3.1\,\mathrm{cm}$ (open circles), (b) isopropanol vapour at $d = 1.1\,\mathrm{cm}$ (full circles) and at $d = 3.1\,\mathrm{cm}$ (open circles), and (c) n-butanol vapour at $d = 1.1\,\mathrm{cm}$ (full circles) and at $d = 3.1\,\mathrm{cm}$ (open circles), and (d) comparison of Paschen curves for alcohols that we studied at $d = 1.1\,\mathrm{cm}$. Paschen curve for ethanol is taken from our previous publication [31].

the same time we did not pursue adjustments of the innermost impedance that would require redesigning the experiment to stabilize the discharge [42,43]. Spatial profiles of emission from the discharges recorded along with breakdown data confirm that even at the highest pressures for the *pd*s covered here there is no evidence of a transition to the streamer discharge.

3.2 Axial profiles of emission

We have recorded axial distributions of light intensities integrated over the visible spectral range at different values of *pd* – from 0.10 Torr cm to 0.70 Torr cm. Axial distributions of emission in the low-current limit of the $V - A$ characteristics ($\sim 1\,\mu\mathrm{A}$) are shown in Figure 3 for the two electrode gaps 1.1 and 3.1 cm for methanol (Fig. 3a) and for 3.1 cm for discharges in isopropanol and n-butanol (Fig. 3b). Profiles are obtained from 2D side-on images of the discharge (Fig. 3a).

It has been often stated that the anatomy of discharges may be used to reveal information on overall particle kinetics at different conditions [44–48]. In discharges in alcohol vapours as it can be seen in emission profiles in Figure 3, electron induced excitation is responsible for the shape of emission distribution with the typical exponential increase in intensity towards the anode, at highest *pd*s (lowest E/Ns) covered by our measurements. At lower *pd* i.e. higher E/N, even ions may gain enough energy for excitation. Furthermore, charge exchange with neutral

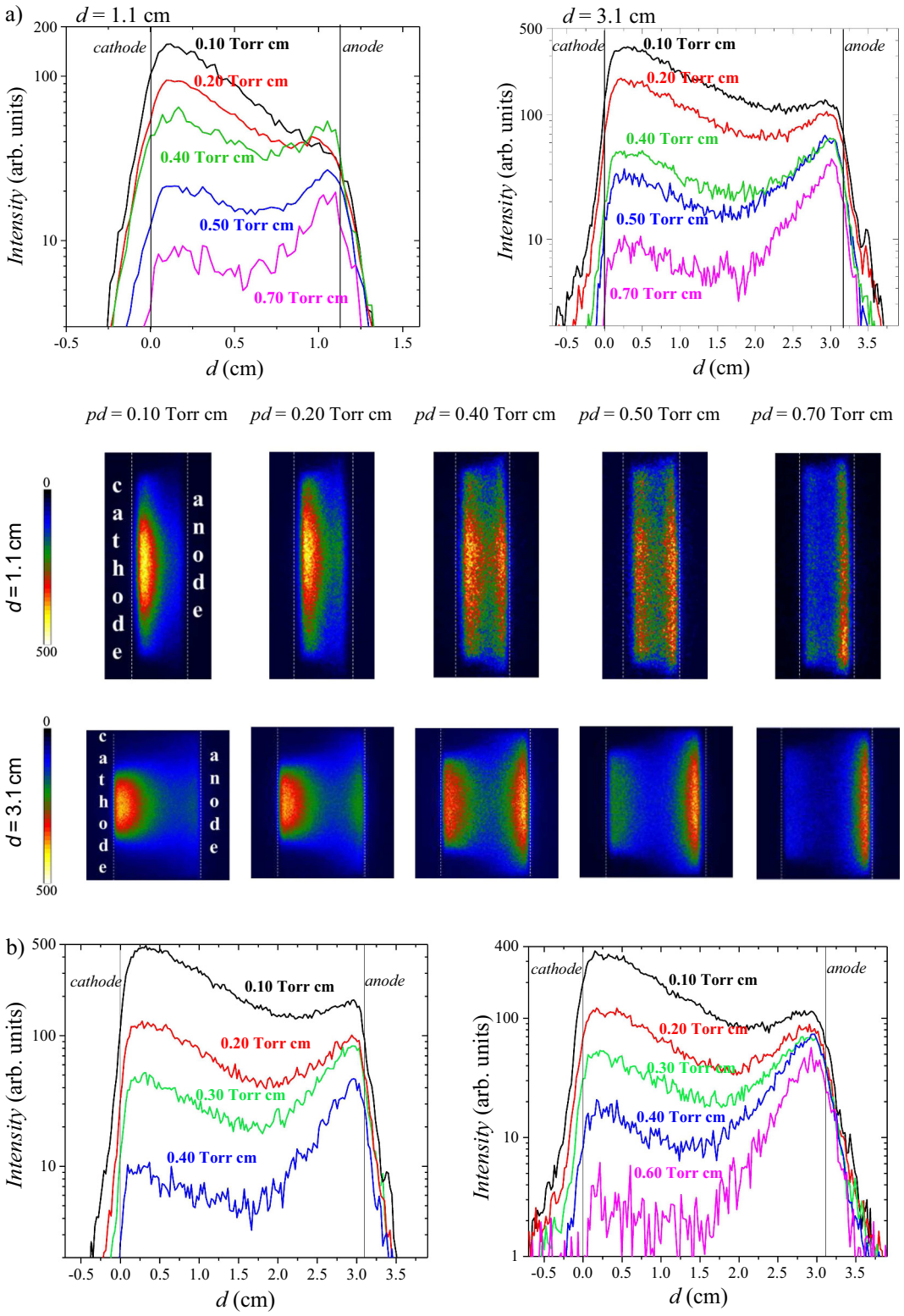

Fig. 3. (a) Axial profiles of emission from discharge in methanol vapour for different values of *pd* (pressure x electrode gap) at electrode gaps: $d = 1.1$ cm and $d = 3.1$ cm. Below the graphs are presented 2D false–colour images of the discharge that correspond to *pd* values at the given electrode gaps showed above. (b) Axial profiles of emission from discharge in isopropanol (left), and n-butanol (right) vapours for different values of *pd* (pressure x electrode gap) at electrode gap $d = 3.1$ cm.

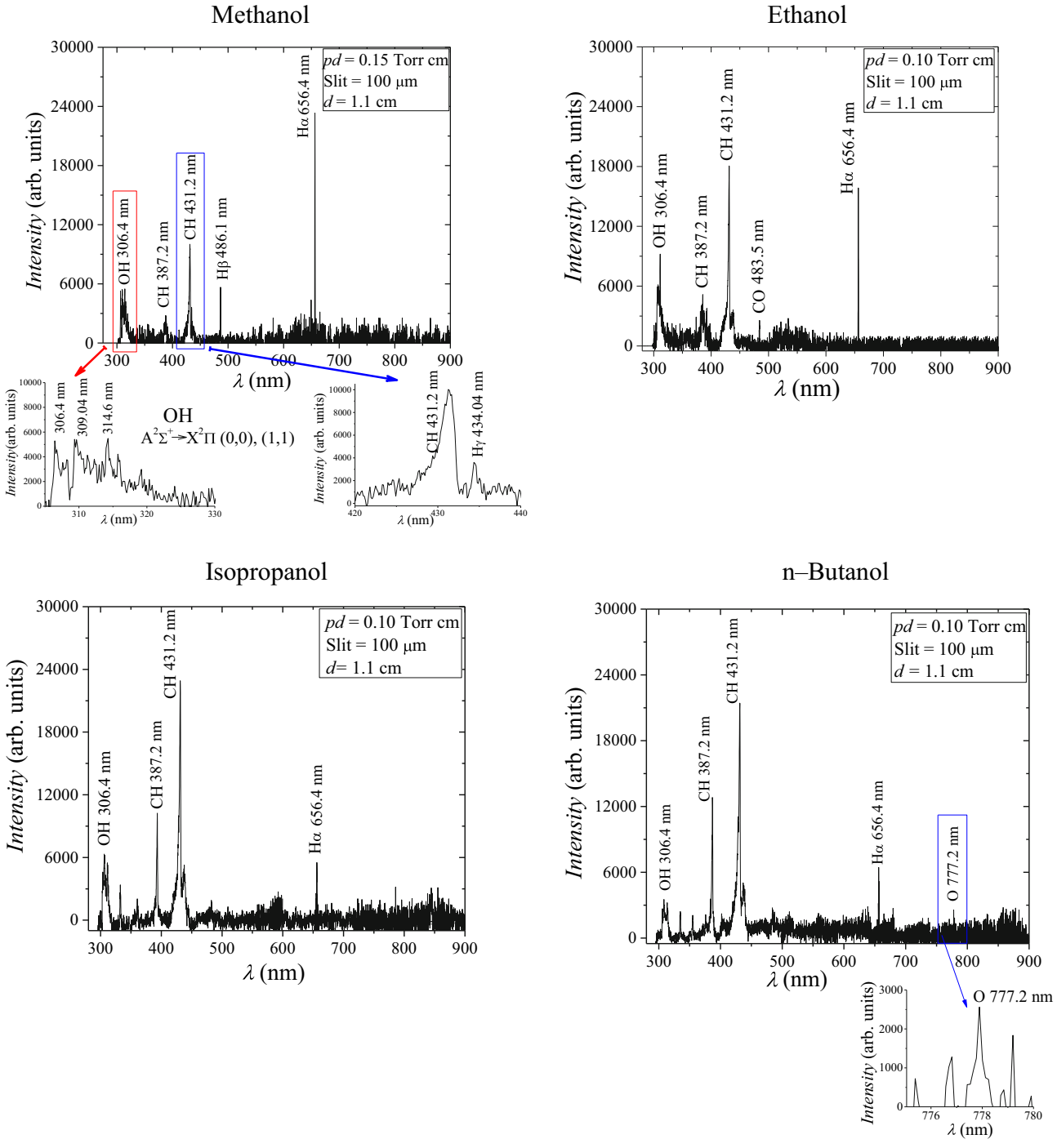

Fig. 4. Emission spectra of discharge in alcohol vapours at low pressure (in the left–hand branch of Paschen curve) and $d = 1.1$ cm. The width of the spectrograph slit was 100 μm.

atoms and molecules may be very efficient, as it has been seen in [45,49,50], so fast neutrals play an important and even dominant role at high E/N. With further increase in E/N contribution of heavy particles increases, which is clearly revealed in Figure 3 through the rising peak of emission close to the cathode. In the range of Paschen minimum, the contribution of heavy particles to excitation is almost the same as the contribution of electrons for all vapours of alcohols presented here. At even lower pressures heavy particles become dominant.

3.3 Spectrally and spatially resolved emission

Optical emission spectra (OES) for discharges in selected alcohols are presented in Figure 4. Here, we repeat the

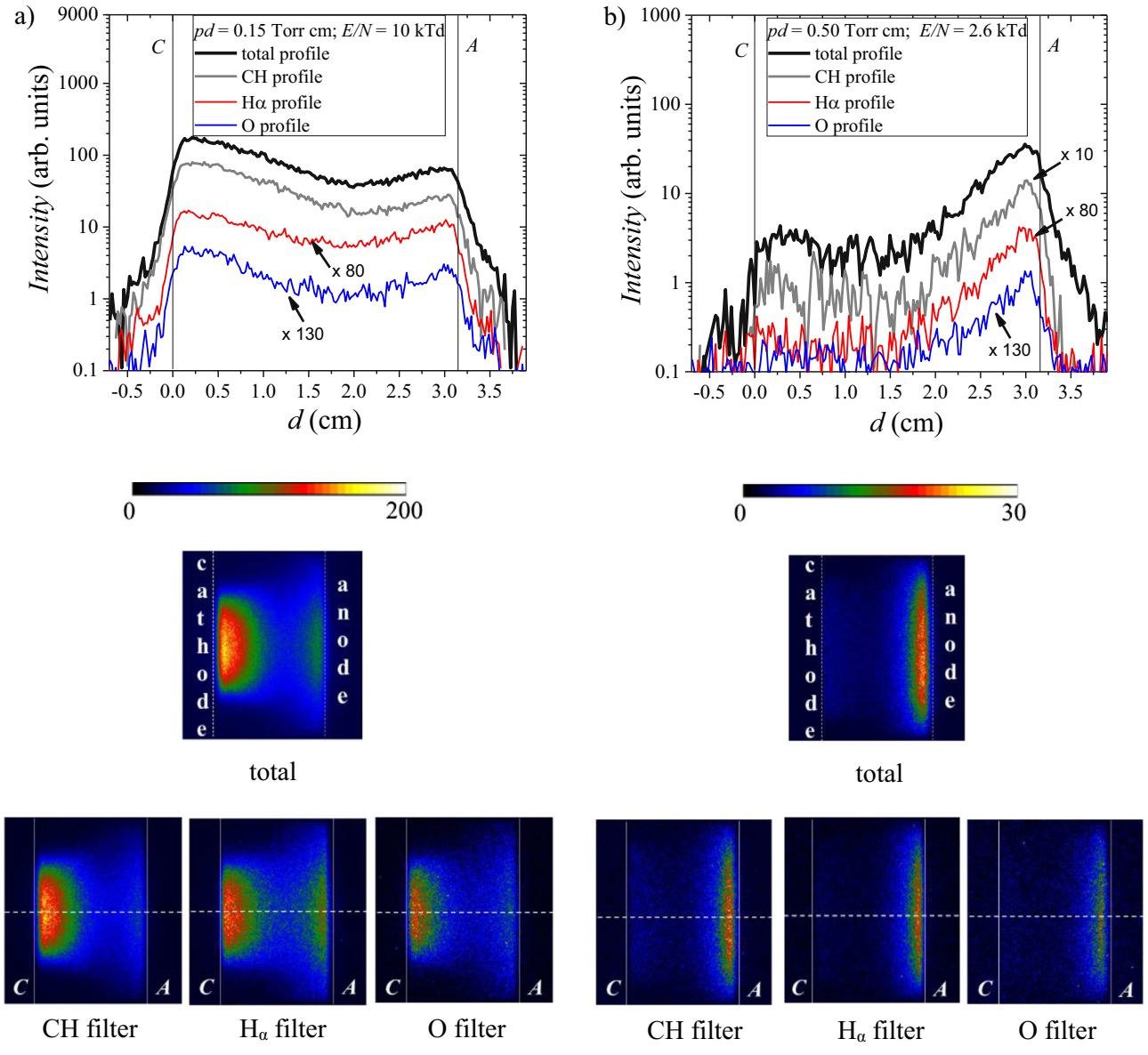

Fig. 5. Axial profiles of emission from discharge in n-butanol vapour at electrode gap $d = 3.1$ cm for two values of pd (pressure x electrode gap): (a) 0.15 Torr cm and E/N (reduced electric field) 10 kTd and (b) 0.50 Torr cm and $E/N = 2.6$ kTd. Emission intensity of selected lines is corrected for the filter transparency and presented at the same intensity scale. Some of the profiles are multiplied by the scaling factor for easier comparison of results. Letters C and A indicate positions of cathode and anode. Axial emission intensity distributions are obtained by extracting the intensities along the horizontal axis shown by the dashed line in 2D images.

ethanol emission spectrum from [31] for comparison with the alcohol spectra presented in this paper.

The spectra were obtained for conditions in the left-hand branch of the Paschen curve, or in other words, at low pressures and at high E/N. All recordings were done at low currents (1 to 3 μA), i.e. for the discharge operating in the Townsend regime, where space charge effects can be neglected. The strongest line for simpler alcohols is H_α, while for the more complex alcohols, that line is subdued, and CH emission is the strongest.

Optical emission spectra measurements were performed in the spectral range from 300 to 900 nm, in which the most intense emissions belong to OH and CH radicals and atoms O and H (Balmer series lines). The detected emission stems from the excited species produced in dissociative excitation of the parent molecule producing H atoms and some heavier excited dissociation fragments (OH, CO and/or CxHy) [31,51–55]. The optical emission spectrum of ethanol vapour discharge was described in detail in [31]. If we look at all recorded OES, it is obvious that emissions originated from OH, CH, and H_α, are the most prominent in the herein studied discharges of alcohol. The emission at 306.4 nm originates from OH radicals [54–57]. On the other hand, the emission of CH radicals comes from two

dominant systems: (1) the $A^2\Delta \rightarrow X^2\Pi$ system, with the band-head at 431.2 nm, and (2) the $B^2\Sigma^- \rightarrow X^2\Pi$ system, with the band-head at 387.2 nm [50–54]. The isopropanol and n-butanol have more carbon content than methanol and ethanol do and contain many more C–H bonds, so CH emission has the highest intensity in these discharges [58].

The recorded optical emission spectra were used to select the appropriate band-pass optical filters for spectrally resolved recordings of spatial emission distributions from discharges. In the case of n-butanol, we used optical filters for extracting emissions at three selected wavelengths: 431.2 nm (CH), 656.4 nm (Hα), and 777.2 nm (O). Figure 5 shows axial profiles of emission from the discharge in n-butanol vapour, obtained for electrode gap of 3.1 cm, in the left part of the Paschen curve at $pd = 0.15$ Torr cm and $E/N = 10$ kTd, and in the right-hand branch of the Paschen curve at $pd = 0.50$ Torr cm and $E/N = 2.6$ kTd. Axial emission profiles are extracted along the horizontal discharge axis from 2D images (white dashed line in Fig. 5).

At $pd = 0.15$ Torr cm (Fig. 5a) the dominant part of emission originates from excitation induced by heavy particles (ions, fast neutrals and metastables but presumably mostly fast neutrals – see Phelps Petrović [45]). That is indicated through the peak of emission close to the cathode [46,47]. Axial profiles of CH (grey line), H_α (red line) and O (blue line) emission follow the integrated emission profiles (black line) (Fig. 5a). The most significant contribution to fast neutral induced emission (i.e. at low pressures and high E/N) comes from the excited CH radical. A less significant contribution to the heavy-particle excitation belongs to O and H species.

With an increase in pressure, (e.g. at $pd = 0.50$ Torr cm, Fig. 5b), the maximum of emission in front of the anode becomes a dominant feature in the profile. The peak of the total emission (black line) near the anode is due to the excitation in electron–neutral collisions. Also, the shapes of CH, H_α, and O profiles (at 0.50 Torr cm, Fig. 5b), reveal that these emissions are the consequence of the electron excitation. On the other hand, at 0.15 Torr cm (Fig. 5a) H and O atoms, and CH radical are excited in collisions with heavy particles.

4 Conclusions

Non-equilibrium discharges in alcohols, either in the liquid or gas phase, have become a very popular area of research, largely because of their wide field of application [1–14,23]. The main obstacles to further understanding of these complex systems lie in the incompleteness and lack of relevant data on elementary processes that exist in the literature [23]. Therefore, we aim to provide information necessary for understanding some of the properties of DC breakdown, low–current and glow discharges in alcohol vapours.

In this paper we present data from experimental studies of the DC breakdown in three alcohol vapours: methanol, isopropanol and n-butanol, at low pressure. Paschen curve that has the lowest breakdown voltage, i.e. the lowest minimum is for n-butanol, at both electrode distances: 1.1 and 3.1 cm. On the other hand, methanol vapour has the highest breakdown voltages. Also, recorded Paschen curves show that minimum shifts towards the lower pressures, higher E/N, for more complex alcohols. The complexity is proportional to the number of atoms in a molecule so with increase in complexity there are more modes for vibrational excitation that causes greater losses requiring breakdown at higher E/N. To the right of the Paschen minimum this is satisfied by increasing the breakdown voltage but to the left of the Paschen minimum the more efficient way to reach higher E/N (i.e. mean energy) is to shift the minimum to the lower values of pd. Thus, the most complex molecule has the higher breakdown voltages to the right of Paschen minimum and the lowest breakdown voltage to the left of Paschen minimum. The dependence of our results on the complexity must have some relationship to the photon induced processes as the dissociation must proceed along the same basic molecular potential curves. However, we were not able to identify the relationship. One could perhaps pursue the relationship between photon induced dissociation/ionization processes and their energy dependence with our observations and see whether some deeper relationship may be defined. In any case such a study should be based on distribution functions and electron scattering cross sections on the side of Paschen curve modelling and understanding of molecular potential curves for photon processes.

Recorded axial profiles of emitted light from low–current discharge reveal that heavy–particles make a significant contribution to breakdown in alcohol vapours, in a wide range of values of pd i.e. E/N. Even at moderate values of reduced electric field E/N, from 3 to 5 kTd, heavy–particle induced processes have a significant role in the discharge. For higher values of E/N they become dominant.

Spatially resolved emission measurements with optical filters show that most of the emission in visible spectral range originates from CH radicals, O, and H atoms, probably mostly through dissociative excitation rather than ground state excitation [59]. Measurements of OES reveal that OH band (head at 306.4 nm), CH band (head at 431.2 nm) and H_α line (656.4 nm) have the largest share in the emission spectrum in the range from 300 to 900 nm, for discharges in all alcohols studied here, while CO (also detected in ethanol discharge), C, and O lines are visible in isopropanol and n-butanol discharges. The measured data provide the basis to describe the breakdown in alcohol vapours, to identify species and elementary processes that participate in these discharges. The obtained results also can enable further progress in modelling of the breakdown in alcohols.

The authors acknowledge support from the Serbian Ministry of Education, Science and Technological Development under project numbers OI 171037 and III 41011.

Author contribution statement

Jelena Sivoš – performed experimental measurements and calculations, analyzed the results and wrote the draft of the manuscript. Dragana Marić – led the studies and interpretation of the results, participated in analysis and discussion of the raw data and the results and participated in revising and writing the paper. Gordana Malović – helped in the analysis of data pertaining to emission properties of studied discharges, in the discussion of the results and in the editing of the manuscript. Zoran Lj. Petrović – defined the plan of research and development of the experimental procedure. He supervised the studies and analysis of the results, organization and finalization of the manuscript.

References

1. G. Petitpas, J.D. Rollier, A. Darmonb, J. Gonzalez-Aguilar, R. Metkemeijer, L. Fulcheri, Int. J. Hydrogen Energy **32**, 2848 (2007)
2. M.G. Sobacchi, A.V. Saveliev, A.A. Fridman, L.A. Kennedy, S. Ahmed, T. Krause, Int. J. Hydrogen Energy **27**, 635 (2002)
3. F. Chen, X. Huang, D. Cheng, X. Zhan, Int. J. Hydrogen Energy **39**, 9036 (2014)
4. B. Wang, B. Sun, X. Zhu, Z. Yan, Y. Liu, H. Liu, Q. Liu, Int. J. Hydrogen Energy **41**, 7280 (2016)
5. R. Dillon, S. Srinivasan, A.S. Aricò, V. Antonucci, J. Power Sources **127**, 112 (2004)
6. M.Z.F. Kamarudin, S.K. Kamarudin, M.S. Masdar, W.R.W. Daud, Int. J. Hydrogen Energy **38**, 9438 (2013)
7. J. Mizeraczyk, M. Jasinski, Eur. Phys. J. Appl. Phys. **75**, 24702 (2016)
8. D.M. Fadzillah, S.K. Kamarudin, M.A. Zainoodin, M.S. Masdar, Int. J. Hydrogen Energy **44**, 3031 (2019)
9. P. Joghee, J. Nekuda Malik, S. Pylypenko, R. O'Hayre, MRS Energy Sustainability **2**, 1 (2015)
10. Q. Wang, X. Wang, Z. Chai, W. Hu, Chem. Soc. Rev. **42**, 8821 (2013)
11. S. Maruyama, R. Kojimaa, Y. Miyauchia, S. Chiashia, M. Kohnob, Chem. Phys. Lett. **360**, 229 (2002)
12. M. Matsushima, M. Noda, T. Yoshida, H. Kato, G. Kalita, T. Kizuki, H. Uchida, M. Umeno, K. Wakita, J. Appl. Phys. **113**, 114304 (2013)
13. A. Ando, K. Ishikawa, H. Kondo, T. Tsutsumi, K. Takeda, T. Ohta, M. Ito, M. Hiramatsu, M. Sekine, M. Hori, Japanese J. Appl. Phys. **57**, 026201 (2018)
14. T. Hagino, H. Kondo, K. Ishikawa, H. Kano, M. Sekine, M. Hori, Appl. Phys. Express **5**, 035101 (2012)
15. N.M. Santhosh, G. Filipič, E. Tatarova, O. Baranov, H. Kondo, M. Sekine, M. Hori, K.K. Ostrikov, U. Cvelbar, Micromachines **9**, 565 (2018)
16. G. Charpak, F. Sauli, Nucl. Instrum. Methods **162**, 405 (1979)
17. S.H. Liebson, Phys. Rev. **72**, 602 (1947)
18. D.J. Grey, R.K. Sood, R.K. Manchanda, Nucl. Instrum. Methods A **527**, 493 (2004)
19. D. Bošnjaković, Z.Lj. Petrović, R.D. White, S. Dujko, J. Phys. D: Appl. Phys. **47**, 435203 (2014)
20. J. Va'vra, Nucl. Instrum. Methods Phys. Res. A **515**, 1 (2003)
21. T.L. Cottrell, I.C. Walker, Trans. Faraday Soc. **61**, 1585 (1965)
22. D. Marić, M. Radmilović-Radenović, Z.Lj. Petrović, Eur. Phys. J. D **35**, 313 (2005)
23. P.J. Bruggeman, M. Kushner, B. Locke, H. Gardeniers, B. Graham, D. Graves, R. Hofman-Caris, D. Marić, J. Reid, E. Ceriani, D. Fernandez Rivas, J. Foster, S. Garrick, Y. Gorbanev, S. Hamaguchi, F. Iza, H. Jablonowski, E. Klimova, F. Krcma, J. Kolb, P. Lukes, Z. Machala, I. Marinov, D. Mariotti, S. Mededovic Thagard, D. Minakata, E. Neyts, J. Pawlat, Z.Lj. Petrović, R. Pflieger, S. Reuter, D. Schram, S. Schroeter, M. Shiraiwa, B. Tarabova, P. Tsai, J. Verlet, T. von Woedtke, K. Wilson, K. Yasui, G. Zvereva, Plasma Sources Sci. Technol. **25**, 053002 (2016)
24. A.V. Phelps, Z.Lj. Petrović, Plasma Sources Sci. Technol. **8**, R21 (1999)
25. D. Marić, N. Škoro, P.D. Maguire, C.M.O. Mahony, G. Malović, Z.Lj. Petrović Plasma Sources Sci. Technol. **21**, 035016 (2012)
26. A.V. Phelps, B.M. Jelenković, Phys. Rev. A **38**, 2975 (1988)
27. J. Sivoš, N. Škoro, D. Marić, G. Malović, Z.Lj. Petrović, J. Phys. D: Appl. Phys. **48**, 424011 (2015)
28. N. Škoro, D. Marić, G. Malović, W.G. Graham, Z.Lj. Petrović, Phys. Rev. E **84**, 055401 (2011)
29. A. von Engel, in *Ionized Gases*, 2nd edn. (Clarendon Press, Oxford, 1965)
30. Y.P. Raizer, in *Gas Discharge Physics* (Springer, Berlin, Germany, 1991)
31. J. Sivoš, D. Marić, N. Škoro, G. Malović, Z.Lj. Petrović, Plasma Sources Sci. Technol. **28**, 055011 (2019)
32. D.A. Scott, A.V. Phelps, Phys. Rev. A **43**, 3043 (1991)
33. D. Marić, M. Savić, J. Sivoš, N. Škoro, M. Radmilović-Radjenović, G. Malović, Z.Lj. Petrović, Eur. Phys. J. D **68**, 155 (2014)
34. V. Stojanović, N. Škoro, J. Sivoš, G. Malović, D. Marić, Z.Lj. Petrović, Modeling emission from water vapor DC discharge at low Pressure, in *28th Summer School and International Symposium on the Physics of Ionized Gases (SPIG) August 29–September 2, 2016, Belgrade, Serbia* (2016), pp. 328–331, http://www.spig2016.ipb.ac.rs/spig2016-book-online.pdf
35. R.C. Weast, in *Handbook of Chemistry and Physics*, 51st edn. (Chemical Rubber Co, Cleveland, Ohio, 1970)
36. D. Marić, G. Malović, Z.Lj. Petrović, Plasma Sources Sci. Technol. **18**, 034009 (2009)
37. Z.Lj. Petrović, A.V. Phelps, Phys. Rev. E **56**, 5920 (1997)
38. Z.Lj. Petrović, N. Škoro, D. Marić, C.M.O. Mahony, P.D. Maguire, M. Radmilović-Radjenović, G. Malović, J. Phys. D: Appl. Phys. **41**, 194002 (2008)
39. T. Kuschel, I. Stefanović, N. Škoro, D. Marić, G. Malović, J. Winter, Z.Lj. Petrović, IEEE Trans. Plasma Sci. **39**, 2692 (2011)
40. D. Marić, N. Škoro, G. Malović, Z.Lj. Petrović, V. Mihailov, R. Djulgerova, J. Phys.: Conf. Ser. **162**, 012007 (2009)
41. I. Stefanovi, T. Kuschel, N. Škoro, D. Marić, Z.Lj Petrović, J. Winter, J. Appl. Phys. **110**, 083310 (2011)
42. A.V. Phelps, Z.Lj. Petrović, B.M. Jelenković, Phys. Rev. E **47**, 2825 (1993)
43. Z.Lj. Petrović, A.V. Phelps, Phys. Rev. E **47**, 2806 (1993)

44. J.H. Ingold, Anatomy of the discharge, in *Gaseous Electronics: Electrical Discharges*, edited by M. Hirsh, H.J. Oskam (Academic Press, New York, 1978), Vol. 1
45. Z.Lj. Petrović, A.V. Phelps, Phys. Rev. E **80**, 016408 (2009)
46. D. Marić, K. Kutasi, G. Malović, Z. Donkó, Z.Lj. Petrović, Eur. Phys. J. D **21**, 73 (2002)
47. Z.Lj. Petrović, Z. Donkó, D. Marić, G. Malović, S. Živanov, IEEE Trans. Plasma Sci. **30**, 136 (2002)
48. D. Marić, P. Hartmann, G. Malović, Z. Donkó, Z.Lj. Petrović, J. Phys. D: Appl. Phys. **36**, 2639 (2003)
49. Z.Lj. Petrović, B.M. Jelenković, A.V. Phelps, Phys. Rev. Lett. **68**, 325 (1992)
50. Z.Lj. Petrović, V. Stojanović, J. Vacuum Sci. Technol. A **16**, 329 (1998)
51. D.S. Levko, A.N. Tsymbalyuk, A.I. Shchedrin, Plasma Phys. Rep. **38**, 913 (2012)
52. F. Poncin-Epaillard, M. Aouinti, Plasmas Polym. **7**, 1 (2002)
53. A. Yanguas-Gil, J.L. Hueso, J. Cotrino, A. Caballero, A.R. González-Elipe, Appl. Phys. Lett. **85**, 4004 (2004)
54. P.G. Reyes, A. Gómez, H. Martínez, O. Flores, C. Torres, J. Vergara, IEEE Trans. Plasma Sci. **44**, 2995 (2016)
55. D.E. Donohue, J.A. Schiavone, R.S. Freund, J. Chem. Phys. **67**, 769 (1977)
56. A.G. Gaydon, in *The Spectroscopy of Flames*, 2nd edn. (Chapman and Hall, London, United Kingdom, 1974)
57. F. Liu, W. Wang, S. Wang, W. Zheng, Y. Wang, J. Electrostat. **65**, 445 (2007)
58. R. Stocker, J. Karl, D. Hein, in *Proc. PSFVIP-3 in Maui, Hawaii, 2001*, (University of Hawaii Maui College, Maui, 2001), F3003, pp. 1–16
59. J. Tennyson, S. Rahimi, C. Hill, L. Tse, A. Vibhakar, D. Akello-Egwel, D.B. Brown, A. Dzarasova, J.R. Hamilton, D. Jaksch, S. Mohr, K. Wren-Little, J. Bruckmeier, A. Agarwal, K. Bartschat, A. Bogaerts, J.P. Booth, M.J. Goeckner, K. Hassouni, Y. Itikawa, B.J. Braams, E. Krishnakumar, A. Laricchiuta, N.J. Mason, S. Pandey, Z.Lj. Petrovic, Yi.-K. Pu, A. Ranjan, S. Rauf, J. Schulze, M.M. Turner, P. Ventzek, J.C. Whitehead, J.-S. Yoon, Plasma Sources Sci. Technol. **26**, 055014 (2017)